

ASSESSMENT OF RNG $k-\epsilon$, SST $k-\omega$ AND REYNOLDS STRESS MODELS FOR NUMERICAL SIMULATION OF DLR SCRAMJET ENGINE

ANUPAM DEBNATH, BIDESH ROY & ABHIJIT SINHA

National Institute of Technology, Aizawl Mizoram, India

ABSTRACT

In recent years, many researchers have used numerical simulation to investigate scramjet engine because, setting up of testing facilities for scramjet engine is very expensive. Completion of simulation work in less time is cost-effective but, it is also important to achieve good outcome from the simulation work. In this context, the use of appropriate turbulent model for the simulation for DLR scramjet engine is a vital aspect. From the available literature, it is seen that many researchers have used Reynolds stress, SST $k-\omega$ and RNG $k-\epsilon$ models in the field of supersonic flow and combustion. Thus, in this study, the primary objective was to find the better turbulence model in between Reynolds stress, SST $k-\omega$ and RNG $k-\epsilon$ models for numerical simulation of DLR scramjet engine. Finally, from the study, it is found that using SST $k-\omega$ model for numerical simulation of DLR scramjet engine results in more accuracy at a lesser computational time.

KEYWORDS: DLR Scramjet Engine, Reynolds Stress, SST $k-\omega$, RNG $k-\epsilon$ & CFD

Received: May 18, 2019; **Accepted:** Jun 08, 2019; **Published:** Jul 19, 2019; **Paper Id.:** IJMPERDAUG2019120

INTRODUCTION

Need of the modern age is to develop reliable and efficient high-speed air breathing propulsion system (i.e. supersonic to hypersonic flight regime), to achieve the goal towards development of space industries, defence industries and easily affordable long-range human transportation system [1]. Turbofan engines are capable of operating up to a speed of Mach 3 and beyond this Mach; turbofan engines lose its functionality [2]. Even, ramjet propulsion systems are also not capable of operating beyond Mach 5. It is due to excess pressure and temperature losses resulting from deceleration of supersonic flow to subsonic inside combustion chamber [2]. In this context, scramjet is one of the best available systems for high speed propulsion even beyond Mach 5 [3]. Development of scramjet engine is very challenging for researchers due to its complex flow phenomena and unstable chemical reaction process in the combustion chamber. Besides this, setting up of testing facilities for scramjet engine is very expensive [2]. The best economical solution for investigation of scramjet engine has attracted the researchers throughout the world towards computational fluid dynamics (CFD).

In order to further develop the scramjet engine, various researchers have implemented several fuel injection techniques [4]. One of the popular injection schemes for scramjet engine is transverse injection of fuel into supersonic cross flow [5, 6]. This results in formation of bow shock which is normal to the supersonic cross flow. This phenomenon increases the pressure loss significantly in the engine, which affects its performance. However, it is found that bow shock wave increases combustion performance by creating a separation zone at downstream of the shock which supports the holding of the flame [7]. Researchers in the recent past have suggested the use of

parallel fuel injection in scramjet engine by using strut-based injector to inject fuel into the core of the supersonic flow. This results in reduction of the effect of normal bow shock that minimize the performance of engine [8, 9]. However, strut-based injection also results in slight drop in mixing performance as compared with transverse injection [8, 9].

Development of various numerical modelling in computational fluid dynamics plays significant role in investigating supersonic combustion precisely with considerable computational cost. Conventionally, developed Reynolds Averaged Navier Stokes (RANS) models are not enough to analyse supersonic combustion accurately. LES (Large eddy simulation) model has a significant achievement in the field of numerical modelling of supersonic combustion, which is capable of predicting quantitative and qualitative outcome of scramjet engine [10, 11]. LES model has been introduced by many scientists, in the process of investigating the operation of strut scramjet engine. It is seen that using LES model for numerical simulation results in reasonably high computational cost and time [1, 2]. However, in recent years, many researchers have used other computational models to investigate scramjet engine. Dinde et al. [12] have numerically investigated scramjet combustor by introducing RNG $k-\epsilon$ turbulence model with finite rate single step chemistry model. The researchers found convincing results of scramjet combustor in regard to H_2 combustion. Later, Luo et al. [13] conducted a numerical investigation on strut scramjet combustor and found that SST $k-\omega$ model is less convincing compared with $k-\epsilon$ for non-reacting flow simulation. SST $k-\omega$ model introduced by Pandey et al. [14] in their simulation work of scramjet combustor observed that performance of scramjet engine is dependent on effective mixing of fuel into air and reduction of pressure losses. The result obtained by Pandey et al. using SST $k-\omega$ model were highly accurate in comparison with available experimental data. Huang et al. [15] numerically examined effects of parametric changes on strut scramjet combustion flow field, and it is highlighted in their research that two step reaction mechanism with SST $k-\omega$ model has slight changes with single step mechanism. From their investigation, it also can be seen that on using SST $k-\omega$ model, the results obtained are very close to the available experimental values. Reynolds stress model for supersonic flow simulation was conducted by Frauholz et al. [16], and they concluded that the model is capable of predicting boundary layer shockwave interaction effectively and effect of grid reduction is invariant of solution outcome. However, in the numerical simulation of strut scramjet engine, Reynolds Stress model has not yet been used. Hence, the primary objective of this paper is to find the better turbulence model in between Reynolds stress, SST $k-\omega$ and RNG $k-\epsilon$ models for numerical simulation of DLR scramjet engine. Moreover, in this paper, the results of all the numerical simulation is compare against the experimental result obtained by Waidmann et al. [17-20] of German aerospace centre (DLR).

COMPUTATIONAL DOMAIN AND GRID GENERATION

Completion of simulation work in less time is cost-effective but, it is also important to achieve good outcome from the simulation work. So, in our present work we have used 2D models with structured mesh for simulation. To design the 2D model and to generate the structured mesh, ICEM of Ansys software is used. In this work, the dimensions of 2D model are kept similar to the experimental model by waidmann et al. [17-20] as shown in Figure 1(a). The 2D model has a length of 340 mm with upper wall diverging at 3° in outward direction. The distance between upper and lower wall at inlet is 50 mm. At the centre of the combustion chamber, a strut of 32mm length and 12° strut angel is positioned at 77mm from the start of the Scramjet engine. Moreover, structured grid size of 325200 elements and Y^+ value of less than 2.5 near the walls is considered for simulation work, which is shown in Figure 1(b) [21]. For grid dependency analysis, results of bottom wall pressure within Scramjet combustor for non-reacting flow are observed which is shown in Figure 2. Primarily, three different grid sizes of 122980, 226340 and 325200 are used in this analysis for three models. In case of Reynolds

Stress model analysis, one more grid size of 424412 is added, as it is observed from Figure 2(c) that there is a significant deviation between obtained results from grid size 226340 and 325200. Comparing grid size of 325200 with others for all three models, no noteworthy change in the simulation results are obtained (i.e. grid independent solution is obtained) [22]. In the generated grid inside the model, all walls are densely meshed in order to properly calculate shockwave boundary layer interaction. Further, dense grid size is also maintained at inlets, outlet and shear layers. In Figure 1(b), the grid pattern that is shown has half of the original grid size for better realization.

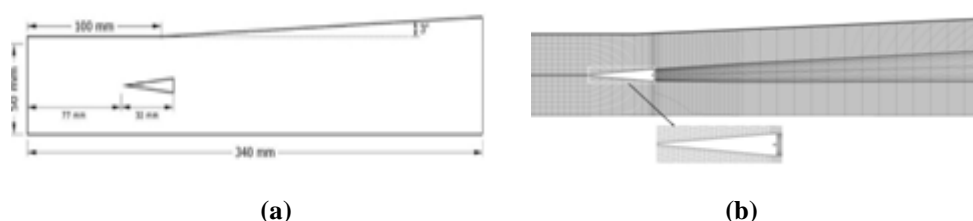


Figure 1: (a) 2D Diagram of DLR Scramjet Engine (b) Grid Pattern for 2D DLR Model

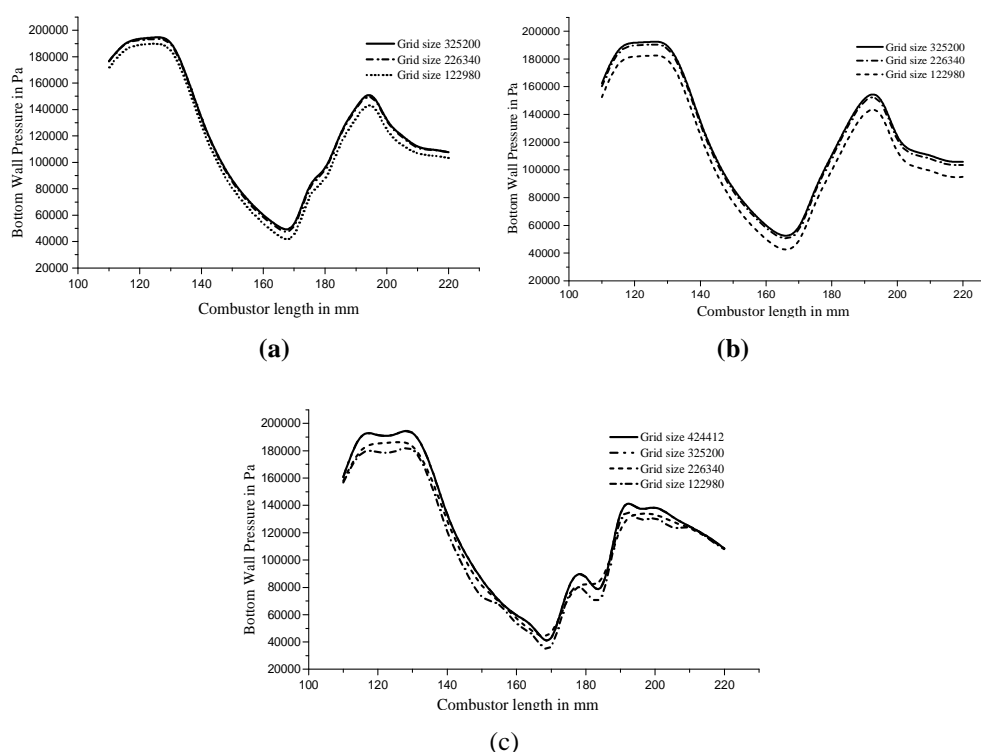


Figure 2: Grid Dependency Test using Bottom Wall Pressure for
(a) RNG $K-\epsilon$, (b) SST $K-\Omega$ and (c) Reynolds Stress Model

NUMERICAL MODELLING AND GOVERNING EQUATIONS

In this study, all the 2D simulations are conducted at steady state condition in Ansys Fluent software. RNG $k-\epsilon$, SST $k-\omega$ and Reynolds Stress model are the three turbulence models, which are selected for the present numerical investigation. For combustion modelling, hybrid chemistry model of finite rate and eddy dissipation are introduced along with the mentioned turbulence models. Single step chemical reaction between hydrogen and oxygen ($2H_2 + O_2 = 2H_2O$) is considered in the present study, to reduce the computational time which is reported by Choubey and Pandey [21]. Description of Transport Equation for all turbulence model used in this work is given below.

RNG k - ε Model

$$\frac{\partial}{\partial t}(\rho k) + \frac{\partial}{\partial x_i}(\rho k u_i) = \frac{\partial}{\partial x_j} \left(a_k \mu_{eff} \frac{\partial k}{\partial x_j} \right) + G_k + G_b - \rho \varepsilon - Y_M + S_k \quad (1)$$

And,

$$\frac{\partial}{\partial t}(\rho \varepsilon) + \frac{\partial}{\partial x_i}(\rho \varepsilon u_i) = \frac{\partial}{\partial x_j} \left(a_\varepsilon \mu_{eff} \frac{\partial \varepsilon}{\partial x_j} \right) + C_{1\varepsilon} \frac{\varepsilon}{k} (G_k + C_{3\varepsilon} G_b) - C_{2\varepsilon} \rho \frac{\varepsilon^2}{k} - R_\varepsilon + S_\varepsilon \quad (2)$$

Where,

G_k, G_b is the turbulence kinetic energy produced due to mean velocity gradient and buoyancy, respectively. Y_M is the ratio of fluctuating dilation to the overall dissipation rate in compressible turbulence. The two terms, a_ε and a_k are inverse effective Prandtl numbers. Further, the user defined terms are represented as S_ε, S_k .

SST k - ω Model

$$\frac{\partial}{\partial t}(\rho k) + \frac{\partial}{\partial x_i}(\rho k u_i) = \frac{\partial}{\partial x_j} \left(\Gamma_k \frac{\partial k}{\partial x_j} \right) + G_k - Y_k + S_k \quad (3)$$

and,

$$\frac{\partial}{\partial t}(\rho \omega) + \frac{\partial}{\partial x_j}(\rho \omega u_j) = \frac{\partial}{\partial x_j} \left(\Gamma_\omega \frac{\partial \omega}{\partial x_j} \right) + G_\omega - Y_\omega + D_\omega + S_\omega \quad (4)$$

Where, G_ω is the representation of ω . Γ_k and Γ_ω is the effective diffusivity of k and ω respectively. Dissipation of k, ω is represented by Y_k, Y_ω . Further, user defined terms are S_k and S_ω .

Reynolds Stress Model

$$\begin{aligned} \frac{\partial}{\partial t}(\rho \overline{u'_i u'_j}) + \frac{\partial}{\partial x_k}(\rho u_k \overline{u'_i u'_j}) = & -\frac{\partial}{\partial x_k} \left[\rho \overline{u'_i u'_j u'_k} + p'(\delta_{kj} \overline{u'_i} + \delta_{ik} \overline{u'_j}) \right] + \frac{\partial}{\partial x_k} \left[\mu \frac{\partial}{\partial x_k} (\overline{u'_i u'_j}) \right] - \rho \left(\overline{u'_i u'_k} \frac{\partial \overline{u'_j}}{\partial x_k} + \overline{u'_j u'_k} \frac{\partial \overline{u'_i}}{\partial x_k} \right) - \\ & \rho \beta (g_i \overline{u'_j \theta} + g_j \overline{u'_i \theta}) + p' \left(\frac{\partial \overline{u'_i}}{\partial x_j} + \frac{\partial \overline{u'_j}}{\partial x_i} \right) - 2\mu \frac{\partial \overline{u'_i}}{\partial x_k} \frac{\partial \overline{u'_j}}{\partial x_k} - 2\rho \Omega_k (\overline{U'_j u'_m} \varepsilon_{ikm} + \overline{u'_i u'_m} \varepsilon_{jkm}) + S_{user} \end{aligned} \quad (5)$$

BOUNDARY CONDITIONS

In this study, supersonic conditions are applied at both air and hydrogen inlet, which is incorporated by pressure far-field condition in Ansys fluent software. For all the simulation, pressure outlet boundary condition is applied at the outlet of the model[23]. All fixed wall including strut is introduced with no slip condition for the simulations. All the values of variable at inlet for air and hydrogen are given in Table 1. The convergence criteria are considered on the basis of mass imbalance test, which is the difference between inflow mass and out flow mass of computational domain ($m_{in} - m_{out}$) [24]. Hence, for all the simulations, mass imbalance up to 0.001 is set as a criterion for convergence.

Table 1: Inflow Parameters for Numerical Simulation of DLR Scramjet Engine

Variables	U (m/s)	Ma	T(K)	P(Pa)	Y _{O2}	Y _{H2}	Y _{H2O}	Y _{N2}
Air	730	2	340	100000	0.232	0	0.032	0.736
Hydrogen	1200	1	232	100000	0	0	0	1

VALIDATION OF THE PRESENT WORK

Experimental results, observed by Waidmann et al. [17-20] are taken as reference to validate the present simulation work. Figure 3(a) shows the Schlieren image of DLR experiment and Figures 3(b), 3(c) and 3(d) display the Mach no contour of cold flow simulation using RNG $k-\epsilon$, SST $k-\omega$ and Reynolds Stress model, respectively.

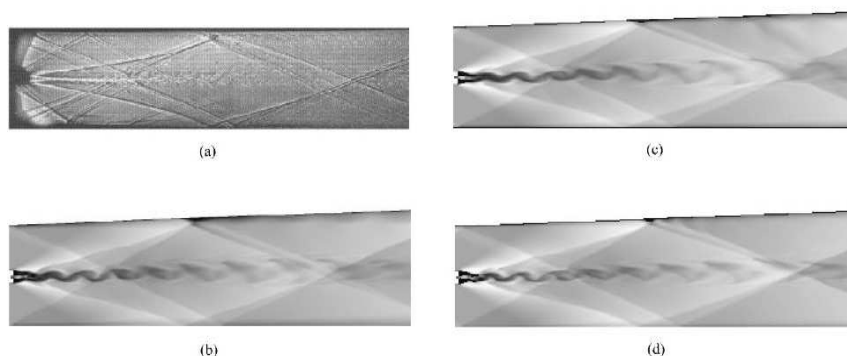


Figure 3: (a) Schlieren Image (b) RNG $K-\epsilon$ Model Predicted Mach No Contour (c) SST $K-\Omega$ Model Predicted Mach No Contour (d) Reynolds Stress Model Predicted Mach No Contour

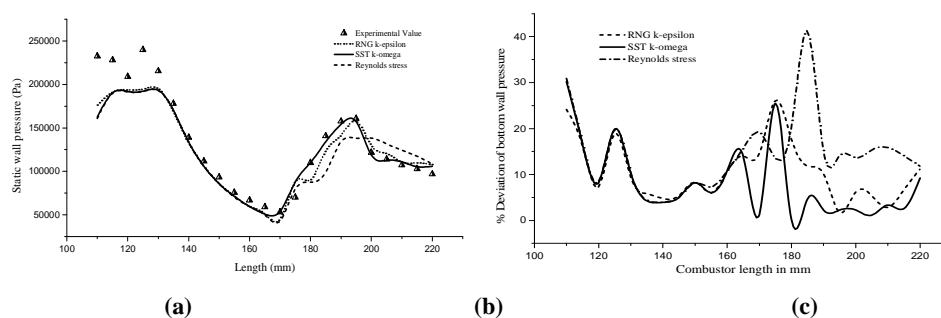


Figure 4: (a) Distribution of Bottom Wall Pressure of DLR Experiment [34-36] with Numerical Calculation (b) Plot of Percentage Deviation for Bottom Wall Pressure of three Models

From figures, it is clearly seen that the shock structure predicted by the simulations and Schlieren image of DLR are similar in structure. Moreover, a comparison between bottom wall pressure distribution obtained from the literature of Waidmann et al. [17-20] and current simulations is also made in this paper which is highlighted in Figure 4. From Figure 4(a), it is observed that pressure distribution predicted along the bottom wall by SST $k-\omega$ model is nearest to the experimental results available in the literature [17-20] in comparison with other turbulence models used in the study. In addition to the above, Figure 4(b) shows the percentage change in prediction of pressure along the bottom wall of DLR scramjet engine by SST $k-\omega$, RNG $k-\epsilon$ and Reynolds Stress models in comparison with the experimental results available in the literature [17-20].

RESULTS AND DISCUSSIONS

In this study, both cold flows as well as reactive flow simulations are conducted using RNG $k-\epsilon$, SST $k-\omega$ and Reynolds Stress model. In case of simulations of reactive flow, an equivalence ratio of 0.136 is maintained which is equal to the equivalence ratio used by Waidmann et al. [17-20] in their experimental investigation of DLR scramjet engine. Solution scheme used in all the numerical simulations is second order upwind, which is highly efficient for capturing shockwave structure and boundary layer accurately.

Contour of Mach No. and static temperature for different turbulence models is shown in Figure 5. On comparing Mach no and static temperature contour for RNG $k-\varepsilon$ and SST $k-\omega$ models, it is observed that there is no significant difference. Both the models predict same static temperature. However, on using Reynolds Stress model, shock structure (in Mach no contour) and temperature contour of different nature are found as compare to RNG $k-\varepsilon$ and SST $k-\omega$ models. Simulation using Reynolds Stress model has predicted highest temperature of 2353K, which is approximately 14% higher than the highest temperature predicted by RNG $k-\varepsilon$ and SST $k-\omega$ models. Reynolds stress model estimates high static temperature, because it predicts the formation of eddies in few regions at the downstream of the flow field which act as flame stabilizer.

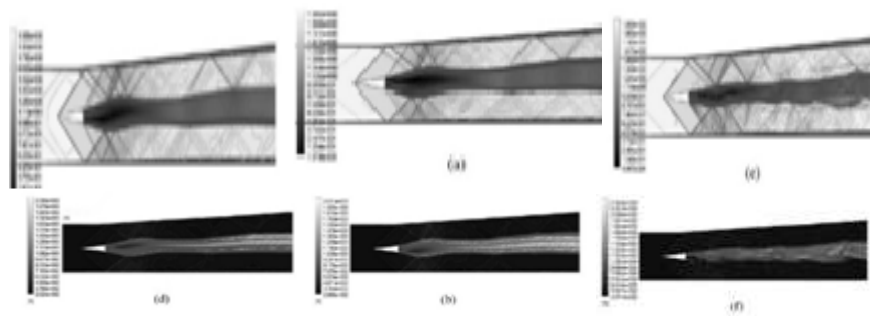


Figure 5: Mach No and Static Temperature Contour For RNG K-E (a, b), SST K-Ω (c, d) and Reynolds Stress(e, f) Models

Mixing efficiency is a very important parameter for the designing of scramjet engine combustor. Good mixing of air and fuel in a short combustor distance provides shorter combustor length, which results in reduction of weight of the combustor [21]. Mixing efficiency at section X, for a non-reacting flow is given by [25].

$$\eta_{mix}(X) = \frac{\int \alpha \rho u Y_{H_2} dA}{m_{H_2}(X)} \quad (6)$$

Where, Area of channel cross section is A, $m_{H_2}(X)$ is mass flow of hydrogen at section X and α is given by

$$\alpha = \begin{cases} 1/\theta & : \theta \geq 1 \\ \theta & : \theta < 1 \end{cases} \quad \text{Here, } \theta \text{ is equivalence ratio.}$$

Figure 6(a), shows mixing efficiency plot along the combustor chamber for different models. Out of these models, RNG $k-\varepsilon$ takes shortest distance(163mm) for complete air-fuel mixing and Reynolds Stress model takes longer distance compared with all other models. Moreover, Figure 6(b) shows the percentage change in prediction of mixing efficiency of DLR scramjet engine by RNG $k-\varepsilon$ and Reynolds Stress models in comparison with SST $k-\omega$ model. The reason for comparing the results of RNG $k-\varepsilon$ and Reynolds Stress models with that of the SST $k-\omega$ model is because, the results predicted by SST $k-\omega$ model is found to be more accurate in term of experimental results which are available in the existing literature. From Figure 8, it is seen that the average deviation in mixing efficiency predicted by RNG $k-\varepsilon$ model is less than Reynolds Stress model. For Reynolds Stress model, higher deviation of 13.85% is observed at a combustor length of 166mm and that for RNG $k-\varepsilon$ model, higher deviation of 23.27% is observed at a combustor length of 157mm.

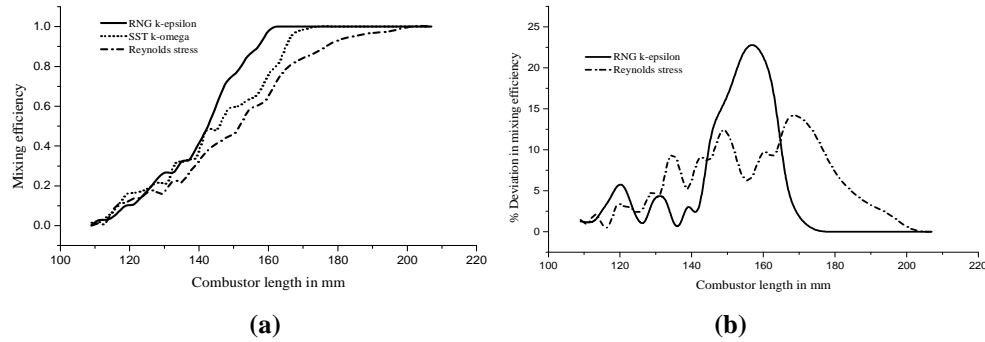


**Figure 6: (a) Mixing Efficiency (η_{mix}) Plot For RNG K-E, SST K- Ω And Reynolds Stress Models
(b) % Deviation In Mixing Efficiency For RNG K- ϵ And Reynolds Stress Models In Comparison With SST K- Ω Model**

Another important parameter in a scramjet engine is combustion efficiency. Study of combustion phenomena in a scramjet engine is very important to finding out the strength of the scramjet engine, and it is determined by combustion efficiency (η_c) [21].

$$\eta_c = 1 - \frac{\int A(x) \rho_{gas} u Y_{H_2} dA}{m_{H_2(inj)}} \quad (7)$$

where, mass flow rate of injected hydrogen is $m_{H_2(inj)}$.

Figure 7(a), shows combustion efficiency plot along the combustor chamber for different models. Out of these models, RNG $k-\epsilon$ and SST $k-\omega$ predicted similar nature of combustion efficiency up to combustor length of 140 mm. Beyond the 140mm length of combustor, RNG $k-\epsilon$ model predicted higher combustion efficiency than SST $k-\omega$ model. RNG $k-\epsilon$ takes shortest distance (163mm) for complete air-fuel mixing and Reynolds Stress model takes longer distance compared with all other models in this study. Furthermore, Figure 7(b) shows the percentage change in prediction of combustion efficiency of DLR scramjet engine by RNG $k-\epsilon$ and Reynolds Stress models in comparison with SST $k-\omega$ model.

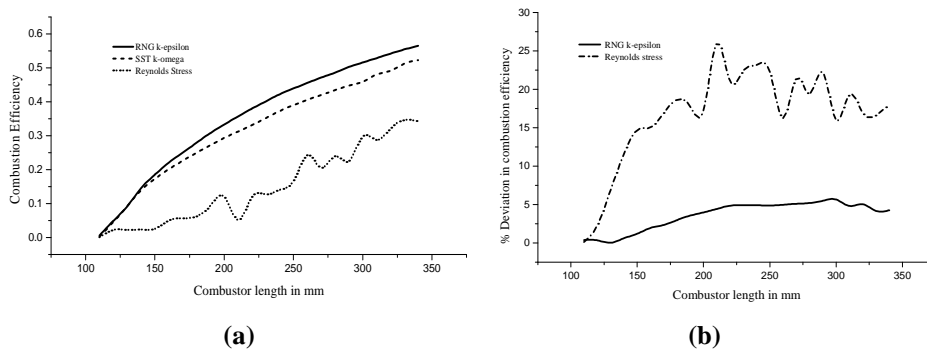


Figure 7: (a) Combustion Performance Plot between RNG k- ϵ , SST k- ω and Reynolds Stress Models (b) % Deviation in Combustion Efficiency for RNG k- ϵ and Reynolds Stress Models in Comparison with SST k- ω Model

The purpose for comparing the results of RNG $k-\epsilon$ and Reynolds Stress models with that of the SST $k-\omega$ model is for the reason that the results projected by SST $k-\omega$ model is found to be more precise in terms of experimental results, which are presented in the available literature. From Figure 10, it is seen that the average deviation in combustion efficiency predicted by RNG $k-\epsilon$ model is less compared with Reynolds Stress model. For Reynolds Stress model, higher deviation of 26.05% is observed at a combustor length of 210mm and that for RNG $k-\epsilon$ model, higher deviation of 5.65% is observed at a combustor length of 166mm.

The simulation in this study is conducted on a workstation equipped with Intel Xenon processor of 8 GB memory. The computational time spend for cold flow simulation using RNG $k-\varepsilon$ and SST $k-\omega$ models were approximately 16 hours and that for using Reynolds Stress model was 31 hours. Whereas, the computational time spends for reactive flow simulation using RNG $k-\varepsilon$ and SST $k-\omega$ models were approximately 36.5 hours and that for using Reynolds Stress model was approximately 74 hours.

CONCLUSIONS

In this study, the primary objective was to find the better turbulence model in between Reynolds stress, SST $k-\omega$ and RNG $k-\varepsilon$ models for numerical simulation of DLR scramjet engine. Base on the results found from the simulations, the following conclusions are drawn.

- The results predicted by SST $k-\omega$ model is found to be more accurate than the results predicted by RNG $k-\varepsilon$ and Reynolds Stress models in comparison with experimental results.
- In reference to the results obtained by using SST $k-\omega$ model, it is seen that the average deviation in mixing and combustion efficiency predicted by RNG $k-\varepsilon$ model is less compared with Reynolds Stress model.
- The computational time required for simulations using RNG $k-\varepsilon$ and SST $k-\omega$ models are substantially less in comparison with Reynolds Stress model.
- Thus, from this study, it can be finally establish that the use of SST $k-\omega$ model for numerical simulation of DLR scramjet engine will provide more accurate result at a lesser computational time.

ACKNOWLEDGEMENTS

The authors gratefully acknowledge National Institute of Technology Mizoram (NIT Mizoram), India for providing all facilities for carrying out this research.

TERMINOLOGY

- DLR - German Aerospace Centre (Deutsches Zentrum für Luft-und Raumfahrt. V.).
- 2D - Two-dimensional, k - Turbulent kinetic energy, SST - Shear stress transport, ω - Turbulent dissipation rate.

REFERENCES

1. Berglund, M., &Fureby, C. (2007). LES of supersonic combustion in a scramjet engine model. *Proceedings of the Combustion Institute*, 31, 2497–2504
2. Fureby, C., Fedina, E., &Tegnér, J(2014). A computational study of supersonic combustion behind a wedge-shaped flameholder. *Shock Waves*, 24, 41–50
3. Curran, E. T. (2001). Scramjet engines: the first forty years. *Journal of Propulsion and Power*, 17 (6), 1138–1148
4. Barber, M. J., Schetz, J. A., &Roe, L. A., (1997). Normal, sonic helium injection through a wedge-shaped orifice into supersonic flow. *Journal of Propulsion and Power*, 13 (2), 257-263
5. Baurle, R. A., Fuller, R. P., White, J. A., Chen, T. H., Gruber, M. R., & Nejad, A. S.(2012). An investigation of advanced fuel injection schemes for scramjet combustion. *American Institute of Aeronautics and Astronautics*, 1- 14

6. Belanger, J., & Hornung, H. G. (1996). Transverse jet mixing and combustion experiments in hypervelocity flows. *Journal of Propulsion and Power*, 12 (1), 186-192
7. Soni, Rahul Kumar, & De, Ashoke (2017). Investigation of strut-ramp injector in a Scramjet combustor: Effect of strut geometry, fuel and jet diameter on mixing characteristics. *Journal of Mechanical Science and Technology*, 31 (3), 1169-1179
8. Dessornes, O., & Jourdain, C. (2012). Mixing enhancement techniques in a scramjet. *American Institute of Aeronautics and Astronautics*, 1-17
9. Seiner, J. M., Dash, S. M., & Kenzakowski, D. C. (2001). Historical survey on enhanced mixing in scramjet engines. *Journal of Propulsion and Power*, 17 (6), 1273-1286
10. Ladiende, F. (ed.), (2010). Special issue on scramjet combustion. *American Institute of Aeronautics and Astronautics*, 48(3)
11. Menon, S., & Fureby, C. (2010). Computational combustion. *Encyclopaedia of Aerospace Engineering*, 1-12
12. Dinde, P., Rajasekaran, A., & Babu, V. (2006). 3D numerical simulation of the supersonic combustion of H₂. *The Aeronautical Journal*, 110, 773-782
13. Luo, Shi-bin, et al. (2011). Investigation of turbulent models for the flow field from a typical strut-based scramjet combustor. *Proceedings of ASME Turbo Expo 2011*, 1-7
14. Pandey, K. M., & Sivasakthivel, T. (2011). CFD analysis of mixing and combustion of a scramjet combustor with a planer strut injector. *International Journal of Environmental Science and Development*, 2 (2), 102-108
15. Wei, H., ZhenGuo1, W., Shi-bin1, L., & Jun, L. (2011). Parametric effects on the combustion flow field of a typical strut-based scramjet combustor. *Chinese Science Bulletin*, 56 (35), 3871-3877
16. Frauholz, S., Bosco, A., Reinartz, B., & Müller, S. (2013). Investigation of Hypersonic Intakes Using Reynolds Stress Modelling and Wavelet-Based Adaptation. *American Institute of Aeronautics and Astronautics*, 52 (12), 2765-2781
17. Waidmann, W., Alff, F., Bohm, M., Brummund, U., Clauss, W., & Oswald, M. (1994). Experimental investigation of hydrogen combustion process in a supersonic combustion ramjet (SCRAMJET). DGLR, Jahrestagung, Erlangen, Germany, p. 629-38.
18. Waidmann, W., Alff, F., Bohm, M., Brummund, U., Clauss, W., & Oswald, M. (1995). Supersonic combustion of hydrogen/air in a scramjet combustion chamber. *Space Technol*, 15 (6), 421-429.
19. Waidmann, W., Brummund, U., & Nuding, J. (1996). Experimental Investigation of Supersonic ramjet combustion (Scramjet). Taylor & Francis, 8th int. symp. On transport phenomena in combustion.
20. Guerra, R., Waidmann, W., & Laible, C. (1991). An experimental investigation of the combustion of a hydrogen jet injected parallel in a supersonic air stream. *American Institute of Aeronautics and Astronautics*, 3rd International Aerospace Planes Conference, Orlando, 91-5102
21. Choubey, G., & Pandey, K. M. (2016). Effect of variation of angle of attack on the performance of two-strut scramjet combustor. *International Journal of Hydrogen Energy*, 1-16
22. Roy, B., Mishra, R. D., Pandey, K. M., Sinha, A., & Deb, B. (2019). Computational and experimental study of swirl flow within SI engine with modified shrouded intake valve. *Computational Fluid Dynamics*, 19 (2), 123-136
23. Anazadehsayed, A., Gerdroodbary, B. M., Amini, Y., & Moradi, R. (2017). Mixing augmentation of transverse hydrogen jet by injection of micro airjets in supersonic crossflow. *Acta Astronautica*, 137, 403-414

24. Zheng, Y., & Zou, J. (2006). *Partially Resolved Numerical Simulation for Supersonic Turbulent Combustion*. 14th AIAA/AHI Space Planes and Hypersonic Systems and Technologies Conference, 2006-8040
25. Baurle, R., Mathur, T., Gruber, M., & Jackson, K. (1998). *A numerical and experimental investigation of a scramjet combustor for hypersonic missile applications*. American Institute of Aeronautics and Astronautics American Institute of Aeronautics and Astronautics, 34th AIAA/ASME/SAE/ASEE joint propulsion conference and exhibit, joint propulsion conferences, 1998-3121